# Lead-free solder alloys: Thermodynamic properties of the (Au + Sb + Sn) and the (Au + Sb) system

Michael Hindler [a,*], Zhongnan Guo [a,b], Adolf Mikula [a]

[a] Institute of Inorganic Chemistry/Material Chemistry, University of Vienna, A-1090 Vienna, Austria
[b] Department of Chemistry, School of Applied Science, University of Science and Technology Beijing, 100083 Beijing, PR China

## ABSTRACT

The thermodynamic properties of liquid (Au–Sb–Sn) alloys were studied with an electromotive force (EMF) method using the eutectic mixture of KCl/LiCl with addition of $SnCl_2$ as a liquid electrolyte. Activities of Sn in the liquid alloys were measured at three cross-sections with constant molar ratios of Au:Sb = 2:1, 1:1, and 1:2 with tin in the concentration range between 5 at.% and 90 at.% from the liquidus of the samples up to 1073 K. The integral Gibbs excess energies and the integral enthalpies at 873 K were calculated by Gibbs–Duhem integration. Additionally liquid Au–Sb alloys have been measured at 913 K with the EMF method as no reliable data for the Gibbs excess energies have been found in literature. The eutectic mixture of KCl/LiCl with addition of $SbCl_3$ has been used as an electrolyte for the measurements. The Gibbs excess energies from the (Au + Sb) system were necessary for the integration of the thermodynamic properties of the ternary (Au + Sb + Sn) system.

© 2012 Elsevier Ltd. Open access under CC BY-NC-ND license.

## 1. Introduction

Many investigations have been done on the field of lead-free solder alloys as it is well known that lead has many toxic effects to the human body. Symptoms of lead poisoning are described *e.g.* in [1–4]. Lead is one of the six substances that are restricted by the RoHS directive, which has been adopted by the European Union in February 2003 [5]. As there are only few replacements available for high-temperature lead-free solders, there are still many exemptions from the RoHS directive for lead containing solders [6]. The (Au + Sn) system shows many possibilities and has been well investigated in the last decades [7–16]. Eutectic $Au_{80}Sn_{20}$ (wt.%) solders are widely used for high-temperature applications for optoelectronics such as laser diodes and photodiodes because of their good creeping properties and high tensile strength. They are also used in flip-chip technology [17]. As the tin-rich eutectic solder is not used in joining technology due to embrittlement of the solder connection [18], the costs for using the gold-rich solder are high. Beside the high costs another disadvantage of the eutectic $Au_{80}Sn_{20}$ (wt.%) solder is that it is only partially able to compensate thermomechanical stress. Hence Sb may be added to Au–Sn solders to improve their thermomechanical behavior and to reduce cost.

Measurements were carried out for three cross-sections with constant ratios of Au–Bi = 2:1, 1:1, and 1:2. The partial thermodynamic properties were calculated from the EMF data. The Gibbs–Duhem integration was carried out to determine the integral thermodynamic properties of the entire ternary system.

Also the (Au + Sb) system has been investigated with the EMF method as no reliable data for the Gibbs excess energies were found. Kameda *et al.* [19] have measured the EMF in 1974 but described their values at antimony content Sb = 20 at.% as unstable. As values for low contents of antimony have high influence on the thermodynamic properties, no definite integration of his activities is possible to get reliable Gibbs excess energies for the starting values needed for the integration of the partial properties of the (Au + Sb + Sn) system. Additionally Kamedás data were described as erroneous in literature by Hayer *et al.* [9] and Kim *et al.* [20]. Enthalpy of mixing values from Kamedás EMF measurements in the (Au + Sb) system were calculated by Hino *et al.* [21] and reported by Okamoto *et al.* [22]. Values were found to be highly exothermic with a strong dependence of temperature. In contrast Hayer *et al.* could proof with a couple of calorimetric measurements [9] over a wide temperature range that the integrated enthalpies of mixing are only slightly exothermic and not temperature dependent. So the EMF data of Kameda are not expected to deliver reliable data for further use.

## 2. Experimental

The Au–Sb–Sn and Au–Sb alloys for the measurements were prepared from high purity metals using tin ingots with a purity

* Corresponding author. Address: Institute of Inorganic Chemistry/Material Chemistry, University of Vienna, Währingerstraße 42, A-1090 Vienna, Austria. Tel.: +43 664 2009637; fax: +43 1 4277 9529.
*E-mail address:* korrosion@gmx.at (M. Hindler).

of 99.999%, a gold sheet with a purity of 99.95% and antimony pieces with a purity of 99.9999%. Tin and antimony were products from Johnson Matthey GmbH, Germany, gold was a product from Ögussa, Austria. Antimony was cleaned by melting under vacuum above quartz wool to remove oxides from the surface. The other metals were used without any further purification. The metals were sealed into quartz capsules under vacuum and melted together at 1073 K. After one week, the alloys were quenched in ice water.

The liquidus of the alloys was then determined by differential thermal analysis (DTA) to identify the temperature range for the emf measurements. Thermal analyses were performed on a 404S DTA instrument (Netzsch, Germany), equipped with type S thermocouples (Pt/Pt-10 wt.% Rh). Samples weighing 200 mg to 300 mg were used for the DTA measurements. The DTA instrument was calibrated using high-purity metals Au, Sb, and Sn as standards to establish internal calibration. Evacuated, sealed quartz tubes were used for the measurements to avoid oxidation of the alloys. Two heating and cooling curves were recorded with a heating and cooling rate of 5 K · min$^{-1}$. For all compositions the mean values of the liquidus were calculated from the two heating curves and are given in table 1.

The activity of tin in the alloys was determined by an EMF method using a liquid electrolyte. The electrolyte consisted of the eutectic mixture of KCl (purity 99.5%) and LiCl (purity 99%) with addition of 0.5 at.% SnCl$_2$ (purity 98%). Cleaning of the electrolyte and assembly of the EMF cell are described in Ref. [23]. A very detailed description of the cell and the setup is also given in Ref. [24]. Measurements were carried out on heating and cooling with a rate of 10 K · h$^{-1}$. The cooling curve was taken to evaluate the thermodynamic properties of this system.

To avoid sublimation of SbCl$_3$ during EMF measurements in the (Au + Sb) system the purified electrolyte, containing the eutectic mixture of LiCl and KCl, was mixed with a small amount of SbCl$_3$, sealed under quartz glass and tempered at 383 K for two month, to get stable compounds, that will not evaporate during the heating phase of the EMF cell. The measurements have been done at 913 K to be sure that the reference was liquid. EMF values were stable for more than one hour. At higher temperatures again the problem of evaporation occurred. As the values at 913 K were sufficient for the integration of the Gibbs excess energy the author did not repeat the measurements at higher temperatures as the experiments were very time consuming.

## 3. Theory and calculations

In order to determine the activities of tin in the (Au + Sb + Sn) system the following cell arrangement was used:
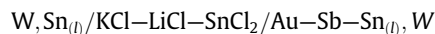
$$W, Sn_{(l)}/KCl-LiCl-SnCl_2/Au-Sb-Sn_{(l)}, W$$

**TABLE 1**
Liquidus temperature of the samples for the Au:Sb = 2:1, 1:1, and 1:2 cross-sections.

| $x_{Sn}$ | Au:Sb = 2:1 Liquidus $T$/K | Au:Sb = 1:1 Liquidus $T$/K | Au:Sb = 1:2 Liquidus $T$/K |
|---|---|---|---|
| 0 | 813 | 723 | 683 |
| 0.050 | 644 | 714 | 748 |
| 0.100 | 679 | 720 | 736 |
| 0.200 | 669 | 718 | 754 |
| 0.300 | 681 | 710 | 738 |
| 0.400 | 673 | 680 | 711 |
| 0.500 | 651 | 630 | 668 |
| 0.600 | 596 | 615 | 633 |
| 0.700 | 571 | 599 | 623 |
| 0.800 | 536 | 524 | 594 |
| 0.900 | 518 | 518 | 526 |

For the determination of the antimony activities in the (Au + Sb) system the cell has been changed to:

$$W, Sb_{(l)}/KCl-LiCl-SnCl_3/Au-Sb_{(l)}, W$$
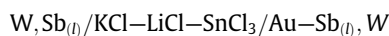
There are several conditions that must be satisfied to achieve accurate EMF measurements. The charge of the electropositive ion Me$^{n+}$ has to be known exactly, and Me$^{n+}$ should be the only charge transfer through the electrolyte and the only reaction on the surface of the electrodes. The electrical conduction through the electrolyte should be purely ionic. No reaction of the electrode and the electrolyte with the apparatus should occur. Concentration changes of the electrodes and the electrolyte during the measurement must be taken into account. During the EMF measurement, no electricity should pass through the cell, which can be achieved by using a voltmeter with an input impedance of more than 10$^{10}$ Ohm. At higher temperatures, for KCl–LiCl at 1123 K, the electrolyte can exhibit some electrical conductivity, so this should be the upper temperature limit for the EMF measurement.

Under reversible conditions the Gibbs free energy change for the reaction in the (Au + Sb + Sn) system is given by

$$\Delta\overline{G_{Sn}} = -z \cdot F \cdot E = RT \cdot \ln a_{Sn}, \tag{1}$$

where $z$ is the number of exchanged electrons, $F$ is the Faraday constant (96,485 C · mol$^{-1}$), $E$ is the electromotive force in volt, $R$ is the universal gas constant (8.3145 J · K$^{-1}$ · mol$^{-1}$), $T$ is the temperature in Kelvin, and $a_{Sn}$ is the thermodynamic activity of tin in the ternary alloy. As reference electrode, pure tin was used. For all measured compositions, the EMF versus temperature curves were straight lines. A least squares fit was used, and the EMF was expressed by the following equation:

$$E/mV = a/mV + b(mV \cdot K^{-1}) \cdot T/K, \tag{2}$$

where $a$ is the ordinate intercept and $b$ is the slope. The resulting linear equations obtained by the least squares method and the standard deviations of the EMF are given in table 2 for the three cross-sections Au:Sb = 2:1, 1:1 and 1:2. From the temperature dependence of $E$ the partial molar enthalpy $\Delta\overline{H_{Sn}}$ and the partial molar entropy $\Delta\overline{S_{Sn}}$ were derived using the following equations:

$$\Delta\overline{H_{Sn}} = z \cdot F\left[E - T\left(\frac{\partial E}{\partial T}\right)\right]_{x,p} = -z \cdot a \cdot F, \tag{3}$$

$$\Delta\overline{S_{Sn}} = z \cdot F\left(\frac{\partial E}{\partial T}\right)_{x,p} = z \cdot b \cdot F. \tag{4}$$

The integral excess Gibbs free energy and the integral enthalpy of mixing were determined by adopting the Gibbs–Duhem equation given by Elliot and Chipman [25] as:

$$\Delta G^{xs} = (1 - x_{Sn})\left[\Delta G^{xs}_{Au-Sb} + \int_0^{x_{Sn}} \frac{\Delta\overline{G^{xs}_{Sn}}}{(1 - x_{Sn})^2}dx_{Sn}\right]_{xAu/xSb}, \tag{5}$$

$$\Delta H = (1 - x_{Sn})\left[\Delta H_{Au-Sb} + \int_0^{x_{Sn}} \frac{\Delta\overline{H_{Sn}}}{(1 - x_{Sn})^2}dx_{Sn}\right]_{xAu/xSb}. \tag{6}$$

$\Delta G^{xs}_{Au-Sb}$ and $\Delta H_{Au-Sb}$ are representing the limiting excess Gibbs energy and enthalpy values of the binary (Au + Sb) system. $x_{Sn}$ is the substance amount fraction of tin in the alloy.

The ternary interaction parameters of the Gibbs excess free energy were calculated using the Redlich–Kister–Muggianu polynomial (equation (7)) given by Ansara and Dupin [26] which was also used for the Gibbs energy and the enthalpies of mixing.

**TABLE 2**
The temperature dependence of the EMF for the Au:Sb = 2:1; 1:1, and 1:2 cross-sections (where $E/mV = (a \pm \Delta a) + (b \pm \triangle b)T$).

| xSn | $a \pm \Delta a$/mV | $b \pm \Delta b$/(mV·K$^{-1}$) |
|---|---|---|
| | *Au:Sb 2:1* | |
| 0.050 | 141.10 ± 0.1830 | 0.1199 ± 0.0002 |
| 0.100 | 120.71 ± 0.5958 | 0.1050 ± 0.0008 |
| 0.200 | 97.69 ± 0.2411 | 0.0614 ± 0.0003 |
| 0.300 | 70.83 ± 0.1563 | 0.0472 ± 0.0002 |
| 0.400 | 44.64 ± 0.1985 | 0.0370 ± 0.0003 |
| 0.500 | 30.72 ± 0.0981 | 0.0271 ± 0.0001 |
| 0.600 | 15.27 ± 0.3169 | 0.0222 ± 0.0004 |
| 0.700 | 5.37 ± 0.1414 | 0.0185 ± 0.0002 |
| 0.800 | 2.28 ± 0.2665 | 0.0098 ± 0.0003 |
| 0.900 | 1.77 ± 0.0567 | 0.0033 ± 0.0001 |
| | *Au:Sb 1:1* | |
| 0.050 | 112.31 ± 0.3463 | 0.1073 ± 0.0004 |
| 0.100 | 97.10 ± 0.2198 | 0.0816 ± 0.0003 |
| 0.200 | 69.76 ± 0.2056 | 0.0652 ± 0.0003 |
| 0.300 | 51.46 ± 0.1989 | 0.0498 ± 0.0003 |
| 0.400 | 36.84 ± 0.0969 | 0.0341 ± 0.0001 |
| 0.500 | 23.39 ± 0.0837 | 0.0281 ± 0.0001 |
| 0.600 | 7.71 ± 0.1588 | 0.0296 ± 0.0002 |
| 0.700 | 5.80 ± 0.0334 | 0.0164 ± 0.0000 |
| 0.800 | −2.19 ± 0.0588 | 0.0179 ± 0.0001 |
| 0.900 | −1.06 ± 0.0649 | 0.0071 ± 0.0001 |
| | *Au:Sb 1:2* | |
| 0.050 | 73.85 ± 0.1638 | 0.1202 ± 0.0002 |
| 0.100 | 73.46 ± 0.2429 | 0.0853 ± 0.0003 |
| 0.200 | 50.63 ± 0.2271 | 0.0692±0.0003 |
| 0.300 | 37.63 ± 0.1493 | 0.0510 ± 0.0002 |
| 0.400 | 27.00 ± 0.2900 | 0.0380 ± 0.0004 |
| 0.500 | 20.96 ± 0.2265 | 0.0228 ± 0.0003 |
| 0.600 | 9.65 ± 0.4319 | 0.0208 ± 0.0006 |
| 0.700 | 7.14 ± 0.2108 | 0.0109 ± 0.0003 |
| 0.800 | 0.12 ± 0.1191 | 0.0130 ± 0.0002 |
| 0.900 | 2.05 ± 0.1793 | 0.0029 ± 0.0002 |

$$\Delta G = \sum_i \sum_{j>i} \left[ x_i x_j \sum_v L_{i:j}^{(v)} \left( x_i - x_j \right)^v \right] + x_A x_B x_C$$
$$\times \left( M_{A:B:C}^{(0)} x_A + M_{A:B:C}^{(1)} x_B + M_{A:B:C}^{(2)} x_C \right), \tag{7}$$

where $i$ and $j$ are equal 1, 2 and 3 representing the elements A, B and C, in this work Au, Sb and Sn. $L_{i:j}^{(v)}$ ($v = 0.1...$) are the interaction parameters of the binary (Au + Sb), (Au + Sn) and (Sb + Sn) system which can be taken from literature. The last term represents the additional Gibbs excess free energy respectively the additional Gibbs free energy or the additional enthalpy of mixing due to the ternary interactions. With the thermodynamic data for the three cross-sections measured, the excess ternary interaction parameters $M_{A:B:C}^{(\alpha)}$ were evaluated. Using the binary and ternary interaction parameters, the thermodynamic properties of the entire ternary system can be calculated.

## 4. Results and discussion

### 4.1. Au–Sb–Sn

Thirty samples were measured at the Au:Sb = 2:1, 1:1, and 1:2 cross-sections (figure 1). The EMF values showed linear dependence on temperature for all investigated compositions. All curves were expressed by equation (2) and the obtained values are given in table 2. Using equations (1), (3), and (4), the activities of tin, the partial Gibbs free energies, partial enthalpies and partial entropies were calculated and are listed in table 3. figure 2 shows the activities of tin for the measured compositions at 873 K in the ternary system and for the two limiting binary systems (Au + Sn) [27] and (Sb + Sn) [28]. It can be seen that the activity of Sn exhibits a
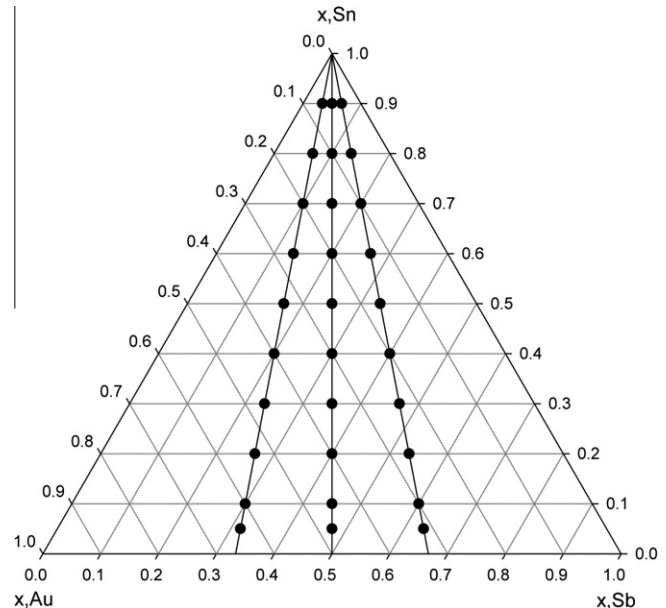


**FIGURE 1.** Measured sections and alloy compositions of the ternary (Au + Sb + Sn) system.

**TABLE 3**
Activities and partial thermodynamic quantities for the Au:Sb = 2:1, 1:1, and 1:2 cross-sections at 873 K.

| $x_{Sn}$ | $a_{Sn}$ | $\Delta \overline{G_{Sn}}$/ (J·mol$^{-1}$) | $\Delta \overline{H_{Sn}}$/ (J·mol$^{-1}$) | $\Delta \overline{S_{Sn}}$/ (J·K$^{-1}$·mol$^{-1}$) |
|---|---|---|---|---|
| | | *Au:Sb 2:1* | | |
| 0.050 | 0.0015 ± 0.0000 | −47427 ± 19 | −27228 ± 35 | 23.14 ± 0.039 |
| 0.100 | 0.0035 ± 0.0000 | −40982 ± 68 | −23293 ± 115 | 20.26 ± 0.154 |
| 0.200 | 0.0179 ± 0.0001 | −29195 ± 29 | −18851 ± 47 | 11.85 ± 0.058 |
| 0.300 | 0.0509 ± 0.0001 | −21620 ± 17 | −13668 ± 30 | 9.11 ± 0.039 |
| 0.400 | 0.1293 ± 0.0004 | −14847 ± 21 | −8614 ± 38 | 7.14 ± 0.058 |
| 0.500 | 0.2356 ± 0.0004 | −10493 ± 12 | −5928 ± 19 | 5.23 ± 0.019 |
| 0.600 | 0.3980 ± 0.0019 | −6687 ± 35 | −2947 ± 61 | 4.28 ± 0.077 |
| 0.700 | 0.5643 ± 0.0010 | −4153 ± 14 | −1036 ± 27 | 3.57 ± 0.039 |
| 0.800 | 0.7497 ± 0.0030 | −2091 ± 29 | −440 ± 51 | 1.89 ± 0.058 |
| 0.900 | 0.8837 ± 0.0007 | −897 ± 6 | −342 ± 11 | 0.64 ± 0.019 |
| | | *Au:Sb 1:1* | | |
| 0.050 | 0.0042 ± 0.0000 | −39749 ± 37 | −21672 ± 67 | 20.71 ± 0.077 |
| 0.100 | 0.0114 ± 0.0000 | −32484 ± 19 | −18737 ± 42 | 15.75 ± 0.058 |
| 0.200 | 0.0345 ± 0.0001 | −24445 ± 21 | −13462 ± 40 | 12.58 ± 0.058 |
| 0.300 | 0.0801 ± 0.0002 | −18320 ± 17 | −9930 ± 38 | 9.61 ± 0.058 |
| 0.400 | 0.1702 ± 0.0002 | −12854 ± 10 | −7109 ± 19 | 6.58 ± 0.019 |
| 0.500 | 0.2797 ± 0.0008 | −9247 ± 8 | −4514 ± 16 | 5.42 ± 0.019 |
| 0.600 | 0.4099 ± 0.0009 | −6474 ± 15 | −1488 ± 31 | 5.71 ± 0.039 |
| 0.700 | 0.5858 ± 0.0002 | −3882 ± 2 | −1119 ± 64 | 3.16 ± 0.000 |
| 0.800 | 0.6996 ± 0.0006 | −2593 ± 6 | 423 ± 11 | 3.45 ± 0.019 |
| 0.900 | 0.8723 ± 0.0007 | −992 ± 6 | 205 ± 13 | 1.37 ± 0.019 |
| | | *Au:Sb 1:2* | | |
| 0.050 | 0.0086 ± 0.0000 | −34500 ± 14 | −14251 ± 32 | 23.19 ± 0.039 |
| 0.100 | 0.0196 ± 0.0001 | −28545 ± 19 | −14176 ± 47 | 16.46 ± 0.058 |
| 0.200 | 0.0522 ± 0.0001 | −21428 ± 17 | −9770 ± 44 | 13.35 ± 0.058 |
| 0.300 | 0.1126 ± 0.0002 | −15853 ± 12 | −7261 ± 29 | 9.84 ± 0.039 |
| 0.400 | 0.2019 ± 0.0009 | −11612 ± 33 | −5210 ± 56 | 7.33 ± 0.077 |
| 0.500 | 0.3374 ± 0.0012 | −7886 ± 25 | −4045 ± 44 | 4.40 ± 0.058 |
| 0.600 | 0.4775 ± 0.0032 | −5366 ± 48 | −1862 ± 83 | 4.01 ± 0.116 |
| 0.700 | 0.6422 ± 0.0023 | −3214 ± 23 | −1378 ± 41 | 2.10 ± 0.058 |
| 0.800 | 0.7372 ± 0.0014 | −2213 ± 14 | −23 ± 23 | 2.51 ± 0.039 |
| 0.900 | 0.8854 ± 0.0014 | −884 ± 12 | 699 ± 35 | 2.47 ± 0.039 |

very strong negative deviation from the Raoult's law both in the binary (Au + Sn) system and the ternary (Au + Sb + Sn) system. The deviation becomes less negative from the Au-rich to the Sb-rich cross-section.
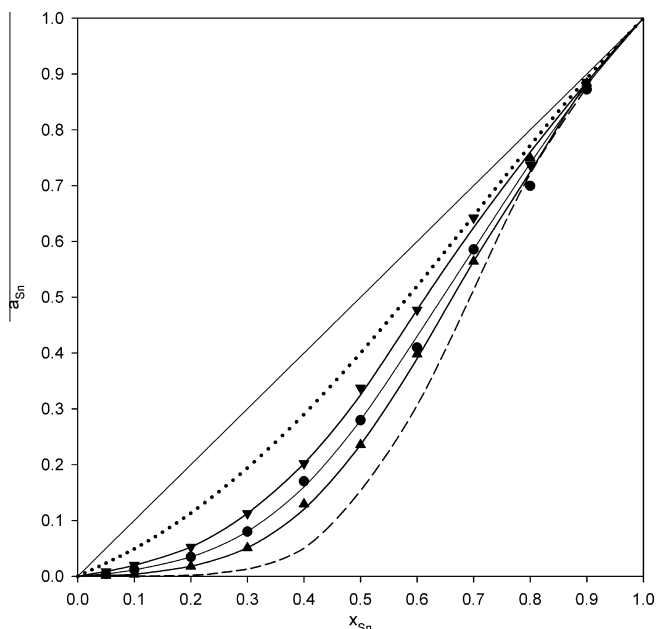
FIGURE 2. Activity curves of Sn for the three cross-sections and the two binary systems at 873 K: ▲Au:Sb = 2:1; ●Au:Sb = 1:1; ▼Au:Sb = 1:2; –– Au–Sn [26]; …Sb–Sn [27].



FIGURE 4. Integral Gibbs free energy for the three cross-sections at 873 K: ▲ Au:Sb = 2:1; ● Au:Sb = 1:1; ▼ Au:Sb = 1:2.

The integral excess Gibbs energies and integral enthalpies of mixing were calculated by using equations (5) and (6). The integration was carried out along three cross-sections. The starting values for $\Delta G^{xs}_{Au-Sb}$ and $\Delta H_{Au-Sb}$ were taken from own measurements and Hayer $et$ $al.$ [9], respectively. The integral thermodynamic properties at 873 K for $\Delta G^{xs}$, $\Delta G$ and $\Delta H$ for the three cross-sections are plotted in figures 3 to 5, respectively. The values are given in table 4. All these three thermodynamic quantities become less negative
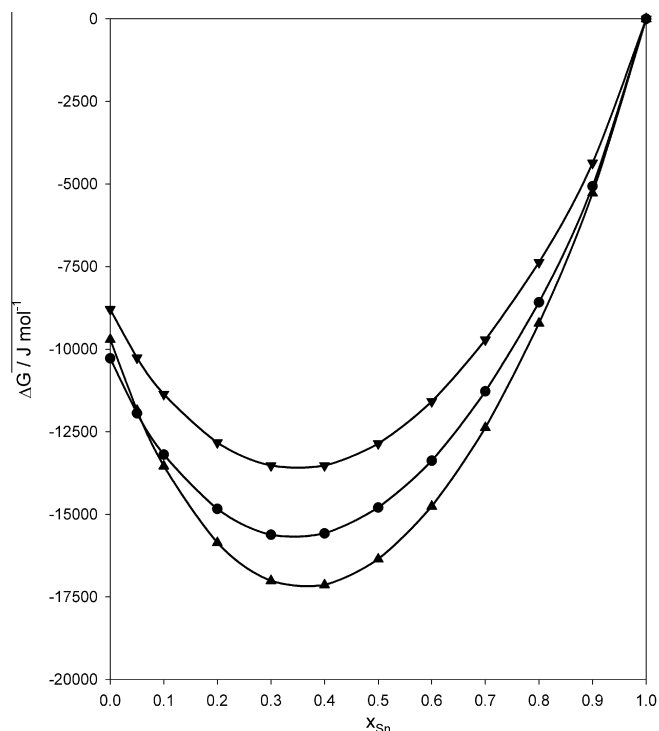
from the Au-rich side (Au:Sb = 2:1) to the Sb-rich side (Au:Sb = 1:2).

The binary and ternary interaction parameters at 873 K for the integral Gibbs excess free energies, the Gibbs free energies and the enthalpies of mixing were calculated with equation (7) and are listed in tables 5 to 7, respectively. The binary data for the Gibbs
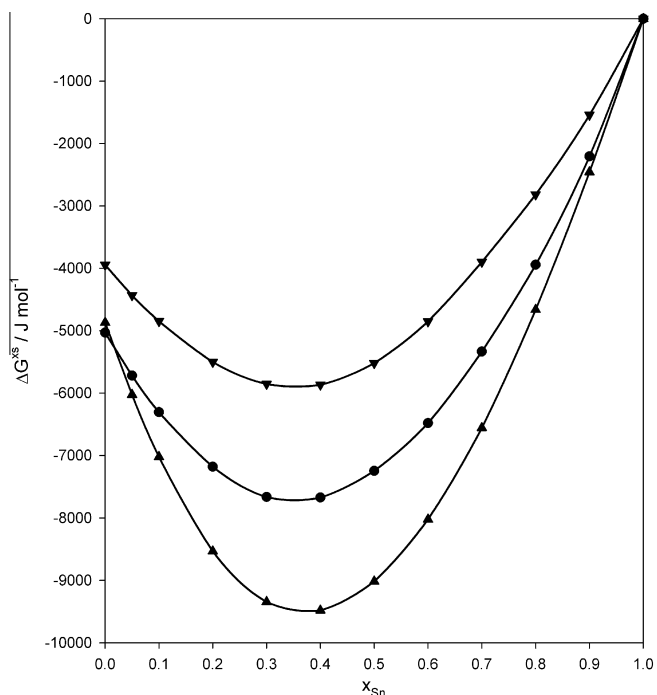


FIGURE 3. Integral excess Gibbs free energy for the three cross-sections at 873 K: ▲ Au:Sb = 2:1; ● Au:Sb = 1:1; ▼ Au:Sb = 1:2.
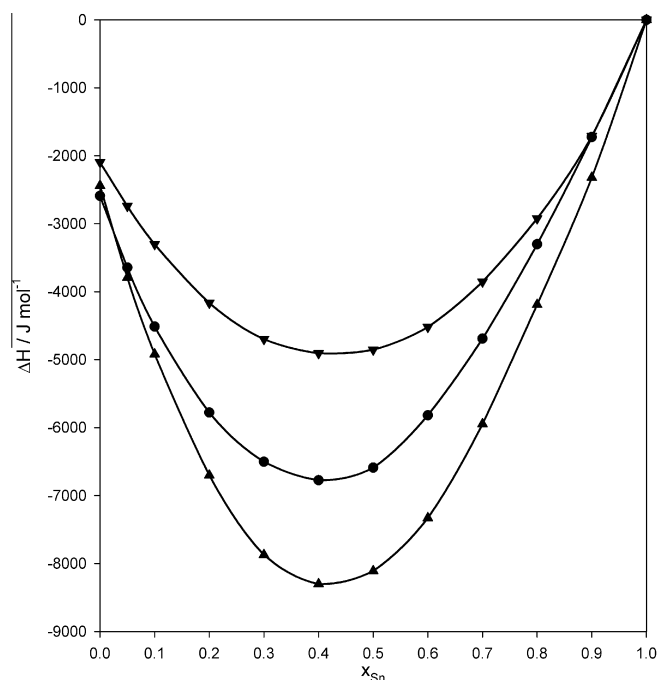


FIGURE 5. Integral enthalpy of mixing for the three cross-sections at 873 K: ▲ Au:Sb = 2:1; ● Au:Sb = 1:1; ▼ Au:Sb = 1:2.

**TABLE 4**
Calculated integral thermodynamic properties for the Au:Sb = 2:1, 1:1, and 1:2 cross-sections at 873 K.

| $x_{Sn}$ | $\Delta G/(J \cdot mol^{-1})$ | $\Delta G^{xs}/(J \cdot mol^{-1})$ | $\Delta H/(J \cdot mol^{-1})$ | $\Delta S/(J \cdot K^{-1} \cdot mol^{-1})$ |
|---|---|---|---|---|
| | | *Au:Sb 2:1* | | |
| 0 | −9706 ± 44 | −4868 ± 44 | −2437 ± 200 [9] | 8.33 ± 0.17 |
| 0.100 | −11854 ± 7 | −6024 ± 7 | −3792 ± 191 | 9.23 ± 0.21 |
| 0.200 | −13539 ± 51 | −7022 ± 51 | −4918 ± 185 | 9.88 ± 0.15 |
| 0.200 | −15863 ± 160 | −8534 ± 160 | −6700 ± 173 | 10.50 ± 0.01 |
| 0.300 | −17013 ± 229 | −9345 ± 229 | −7870 ± 156 | 10.47 ± 0.08 |
| 0.400 | −17139 ± 266 | −9482 ± 266 | −8300 ± 139 | 10.12 ± 0.15 |
| 0.500 | −16358 ± 276 | −9017 ± 276 | −8108 ± 120 | 9.45 ± 0.18 |
| 0.600 | −14756 ± 263 | −8023 ± 263 | −7329 ± 105 | 8.51 ± 0.18 |
| 0.700 | −12377 ± 228 | −6557 ± 228 | −5946 ± 89 | 7.37 ± 0.16 |
| 0.800 | −9219 ± 175 | −4663 ± 175 | −4189 ± 75 | 5.76 ± 0.11 |
| 0.900 | −5278 ± 100 | −2457 ± 100 | −2320 ± 50 | 3.39 ± 0.06 |
| | | *Au:Sb 1:1* | | |
| 0 | −10281 ± 71 | −5032 ± 71 | −2590 ± 200 [9] | 8.81 ± 0.15 |
| 0.050 | −11940 ± 11 | −5720 ± 11 | −3644 ± 172 | 9.50 ± 0.18 |
| 0.100 | −13193 ± 31 | −6306 ± 31 | −4513 ± 166 | 9.94 ± 0.15 |
| 0.200 | −14838 ± 102 | −7181 ± 102 | −5778 ± 152 | 10.38 ± 0.06 |
| 0.300 | −15622 ± 154 | −7666 ± 154 | −6501 ± 139 | 10.45 ± 0.02 |
| 0.400 | −15578 ± 185 | −7674 ± 185 | −6773 ± 122 | 10.09 ± 0.07 |
| 0.500 | −14794 ± 194 | −7248 ± 194 | −6589 ± 105 | 9.40 ± 0.10 |
| 0.600 | −13378 ± 190 | −6481 ± 190 | −5818 ± 90 | 8.66 ± 0.11 |
| 0.700 | −11279 ± 165 | −5336 ± 165 | −4690 ± 80 | 7.55 ± 0.10 |
| 0.800 | −8582 ± 130 | −3944 ± 130 | −3301 ± 63 | 6.05 ± 0.08 |
| 0.900 | −5070 ± 80 | −2207 ± 80 | −27228 ± 35 | 3.83 ± 0.05 |
| | | *Au:Sb 1:2* | | |
| 0 | −8799 ± 81 | −3945 ± 81 | −2096 ± 200 [9] | 7.68 ± 0.14 |
| 0.050 | −10263 ± 44 | −4433 ± 44 | −2740 ± 233 | 8.62 ± 0.22 |
| 0.100 | −11364 ± 11 | −4847 ± 11 | −3301 ± 222 | 9.24 ± 0.24 |
| 0.200 | −12830 ± 46 | −5502 ± 46 | −4165 ± 203 | 9.93 ± 0.18 |
| 0.300 | −13523 ± 91 | −5855 ± 91 | −4698 ± 182 | 10.11 ± 0.10 |
| 0.400 | −13524 ± 121 | −5867 ± 121 | −4905 ± 163 | 9.87 ± 0.05 |
| 0.500 | −12861 ± 135 | −5519 ± 135 | −4854 ± 144 | 9.17 ± 0.01 |
| 0.600 | −11584 ± 136 | −4851 ± 136 | −4519 ± 129 | 8.09 ± 0.01 |
| 0.700 | −9718 ± 13 | −3898 ± 123 | −3853 ± 112 | 6.72 ± 0.01 |
| 0.800 | −7373 ± 97 | −2817 ± 97 | −2922 ± 85 | 5.10 ± 0.01 |
| 0.900 | −4364 ± 63 | −1542 ± 63 | −1711 ± 63 | 3.04 ± 0.00 |

**TABLE 5**
Binary and ternary interaction parameters of the integral Gibbs excess free energy at 873 K.

| Interaction parameter | $\upsilon$ | $G^{xs}/(J \cdot mol^{-1})$ |
|---|---|---|
| $L_{Au-Sb}^{(\upsilon)}$ | 0 | −20,127 |
| | 1 | −6229 |
| | 2 | 2682 |
| $L_{Au-Sn}^{(\upsilon)}$ | 0 | −49,796 |
| | 1 | −13,937 |
| | 2 | 139 |
| $L_{Sb-Sn}^{(\upsilon)}$ | 0 | −6685 |
| | 1 | −41 |
| | 2 | 38 |
| | $\alpha$ | $G^{xs}/(J \cdot mol^{-1})$ |
| $M_{Au-Sb-Sn}^{(\alpha)}$ | 0 | 39,883 |
| | 1 | 9058 |
| | 2 | 13,761 |

**TABLE 6**
Binary and ternary interaction parameters of the integral Gibbs free energy at 873 K.

| Interaction parameter | $\upsilon$ | $G/(J \cdot mol^{-1})$ |
|---|---|---|
| $L_{Au-Sb}^{(\upsilon)}$ | 0 | −41,123 |
| | 1 | −6125 |
| | 2 | −4610 |
| $LAu-Sn^{(\upsilon)}$ | 0 | −69,774 |
| | 1 | −13,771 |
| | 2 | −7915 |
| $L_{Sb-Sn}^{(\upsilon)}$ | 0 | −27,352 |
| | 1 | 41 |
| | 2 | −8844 |
| | $\alpha$ | $G/(J \cdot mol^{-1})$ |
| $M_{Au-Sb-Sn}^{(\alpha)}$ | 0 | 6447 |
| | 1 | −15,095 |
| | 2 | −28,756 |

excess free energy and the Gibbs free energy were taken for the (Au + Sb) system from own measurements, for the (Au + Sn) system from Kameda *et al.* [27] and for the (Sb + Sn) system from Hultgren *et al.* [28]. For the enthalpies of mixing the binary data for (Au + Sb) and the (Au + Sn) system were taken from Hayer *et al.* [29] and for the (Sb + Sn) system from Sommer *et al.* [30]. The iso-excess Gibbs free energy curves, the iso-Gibbs free energy curves and the iso-enthalpy curves are drawn from interaction parameters in figures 6 to 8, respectively. It can be observed that

for the (Au + Sb + Sn) system the minima for $\Delta G^{xs}$ and $\Delta H$ are both located in the binary (Au + Sn) system at about $Au_{56}Sn_{44}$. The minimum of $\Delta G$ can be found at about $Au_{52}Sb_7Sn_{41}$ (at.%) (See figure 9).

### 4.2. Au–Sb

The activity of antimony in six samples was measured at 913 K. EMF values at 913 K are given in table 8. At low and high antimony content measurements are showing less deviation from Raoulťs law. Partial thermodynamic quantities and activities are given in

**TABLE 7**
Binary and ternary interaction parameters of the integral enthalpy of mixing at 873 K.

| Interaction parameter | $v$ | $H/(\text{J} \cdot \text{mol}^{-1})$ |
|---|---|---|
| $L_{\text{Au-Sb}}^{(v)}$ | 0 | $^-$10,360 |
| | 1 | $^-$2303 |
| | 2 | 1428 |
| $L_{\text{Au-Sn}}^{(v)}$ | 0 | $^-$45,934 |
| | 1 | $^-$11,012 |
| | 2 | 2551 |
| $L_{\text{Sb-Sn}}^{(v)}$ | 0 | $^-$5933 |
| | 1 | 936 |
| | 2 | 2408 |
| | $\alpha$ | $H/(\text{J} \cdot \text{mol}^{-1})$ |
| $M_{\text{Au-Sb-Sn}}^{(\alpha)}$ | 0 | 21,012 |
| | 1 | $^-$799 |
| | 2 | 6561 |



**FIGURE 8.** Iso-enthalpy curves $(\text{kJ} \cdot \text{mol}^{-1})$ at 873 K for the ternary (Au + Sb + Sn) system.



**Figure 6.** Iso-excess Gibbs free energy curves $(\text{kJ} \cdot \text{mol}^{-1})$ at 873 K for the ternary (Au + Sb + Sn) system.



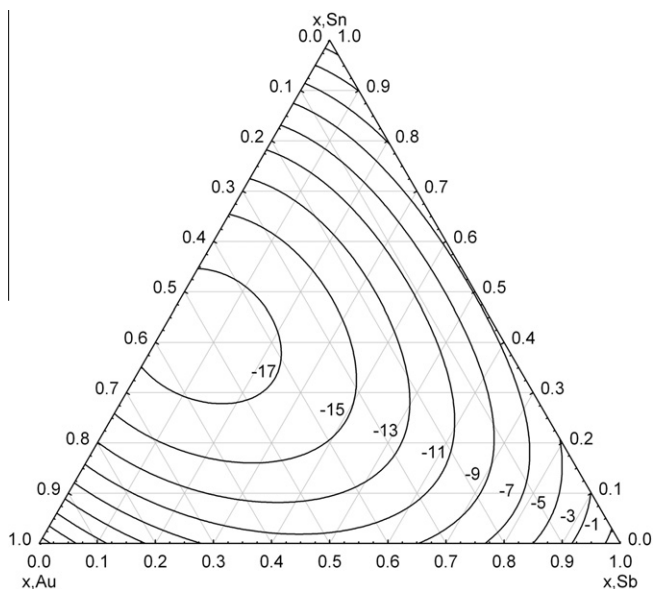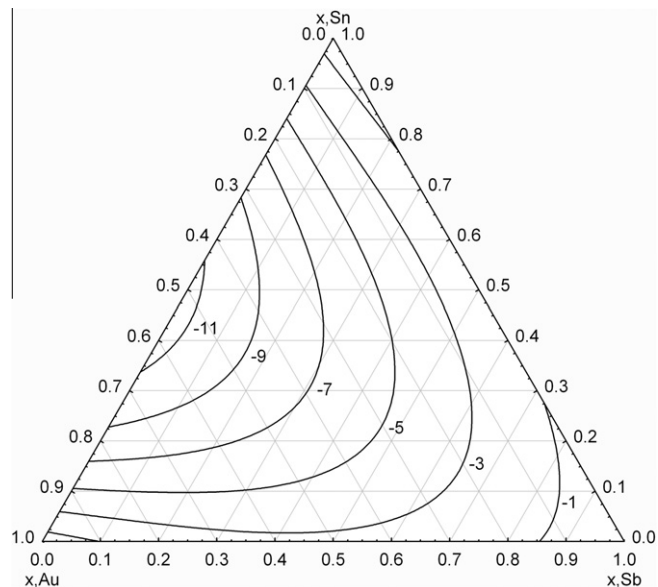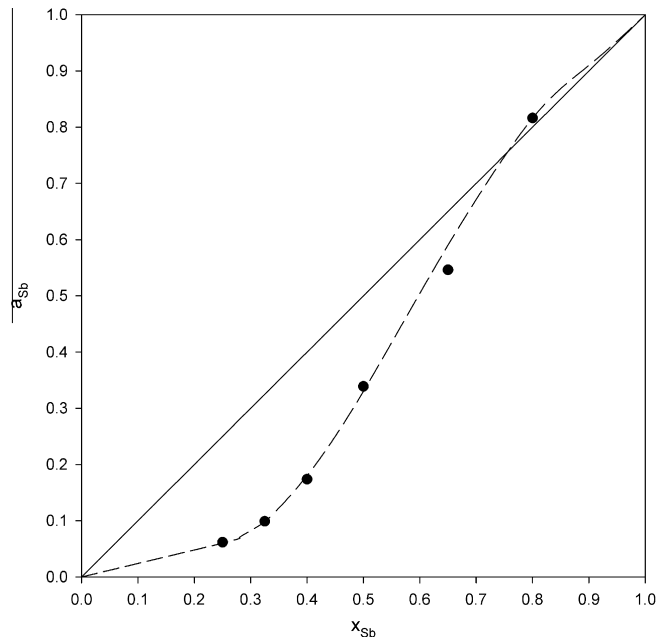**FIGURE 9.** Activity of Sb for the (Au + Sb) system at 913 K.



**FIGURE 7.** Iso-Gibbs free energy curves $(\text{kJ} \cdot \text{mol}^{-1})$ at 873 K for the ternary (Au + Sb + Sn) system.

**TABLE 8**
Experimentally determined EMF data for the (Au + Sb) system at 913 K.

| $x_{\text{Sb}}$ | E/mV |
|---|---|
| 0.250 | 73.2 ± 0.2 |
| 0.325 | 60.8 ± 0.41 |
| 0.400 | 46.0 ± 0.32 |
| 0.500 | 28.4 ± 0.07 |
| 0.650 | 15.9 ± 0.36 |
| 0.800 | 5.34 ± 0.06 |

**TABLE 9**
Activities and partial thermodynamic quantities for the (Au + Sb) system at 913 K.

| $x_{Sb}$ | $a_{Sb}$ | $\Delta\overline{G_{Sb}}/(\text{J} \cdot \text{mol}^{-1})$ |
|---|---|---|
| 0.250 | 0.0613 ± 0.0005 | −21188 ± 58 |
| 0.325 | 0.0984 ± 0.0015 | −17599 ± 119 |
| 0.400 | 0.1731 ± 0.0021 | −13315 ± 93 |
| 0.500 | 0.3386 ± 0.0009 | −8221 ± 20 |
| 0.650 | 0.5454 ± 0.0074 | −4602 ± 104 |
| 0.800 | 0.8158 ± 0.0019 | −1546 ± 14 |

**TABLE 10**
Calculated integral thermodynamic properties for the (Au + Sb) system at 913 K.

| $x_{Sb}$ | $\Delta G/(\text{J} \cdot \text{mol}^{-1})$ | $\Delta G^{xs}/(\text{J} \cdot \text{mol}^{-1})$ |
|---|---|---|
| 0.250 | −8507 ± 27 | −4239 ± 27 |
| 0.325 | −9592 ± 43 | −4806 ± 43 |
| 0.400 | −10232 ± 59 | −5123 ± 59 |
| 0.500 | −10275 ± 67 | −5013 ± 67 |
| 0.650 | −9027 ± 81 | −4113 ± 81 |
| 0.800 | −6260 ± 71 | −2462 ± 71 |

table 9. The integrated Gibbs excess energy and the Gibbs energy are plotted in figures 10 and 11. The values are given in table 10. Results show a minimum for the Gibbs excess energy at about Au$_{57}$Sb$_{43}$ (at.%) with −5.1 kJ · mol$^{-1}$. The minimum for the Gibbs energy can be observed at Au$_{54}$Sb$_{46}$ with −10.3 kJ · mol$^{-1}$.

## 5. Conclusion

The activity of tin for the ternary (Au + Sb + Sn) system was measured by electromotive force method and the thermodynamic data of the liquid alloys was obtained. This is the first report of thermodynamic data on the ternary (Au + Sb + Sn) system by the EMF method. The (Au + Sb) system was measured to obtain starting values for the integration of the Gibbs excess free energy in the (Au + Sb + Sn) system. The results of these investigations can be of great use for the assessment of the phase equilibria, for the design of new lead-free solders, and also for the prediction of some physical and chemical properties.
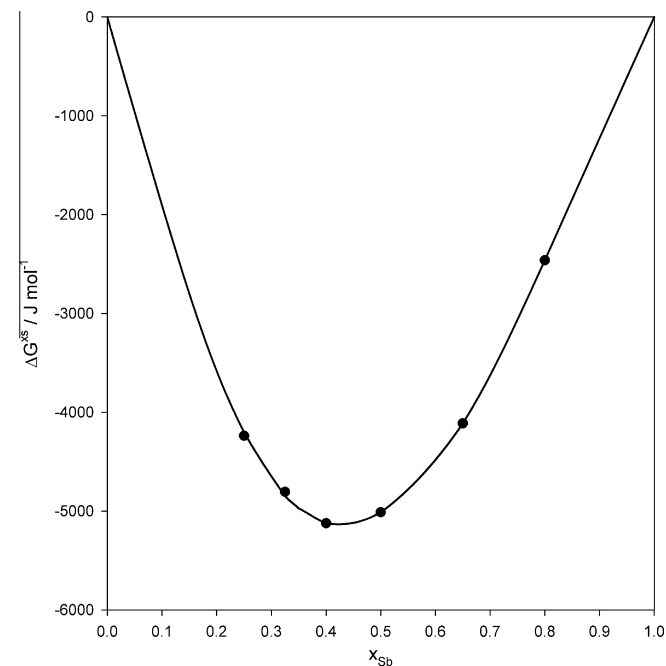
## Acknowledgement

FIGURE 10. Integral excess Gibbs free energy for the (Au + Sb) system at 913 K.
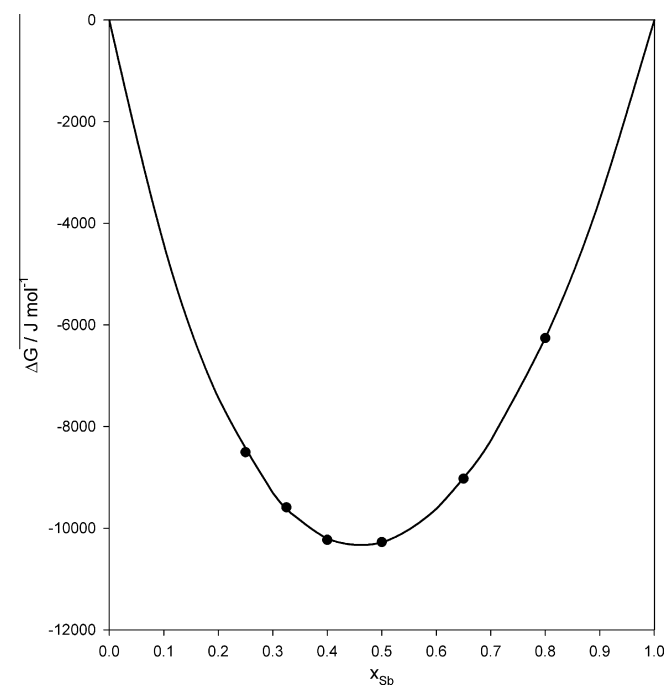


FIGURE 11. Integral Gibbs free energy for the (Au + Sb) system at 913 K.

## References

[1] M. Mycyk, D. Hryhorczuk, Y. Amitai, in: T.B. Erickson, W.R. Ahrens, S. Aks, L. Ling, Pediatric Toxicology: Diagnosis and Management of the Poisoned Child. McGraw-Hill Professional 2005.
[2] L. Patrick, Alternative Med Rev: J Clinical Therapeutic 11 (2006) 2–22.
[3] J.M. Pearce, Eur. Neurol. 57 (2007) 118–119.
[4] J.C. Merrill, J.J.P. Morton, S.D. Soileau, in: A.W. Hayes (Ed.), Principles and Methods of Toxicology, fifth ed., CRC Press, 2007.
[5] The European parliament and the council of the European union, Official Journal of the European Union L 37 (2003) 19–23.
[6] The European parliament and the council of the European union, Official Journal of the European Union L 251 (2010) 28–34.
[7] K. Kameda, S. Sakairi, Y. Yoshida, Nippon Kinzoku Gakkaishi 41 (1977) 950–955.
[8] S.M. Howard, J.P. Hager, Metall. Trans. B 9 (1978) 51–59.
[9] E. Hayer, K.L. Komarek, J.P. Bros, M. Gaune-Escard, Z. Metallkd. 72 (1981) 109–115.
[10] P.Y. Chevalier, Thermochim. Acta 130 (1988) 1–13.
[11] C. Kallmayer, D. Lin, J. Kloeser, H. Oppermann, E. Zakel, H. Reichl, H. Leicht, IEEE/CPMT 17 (1995) 20–28.
[12] D.G. Ivey, Micron 29 (1998) 281–287.
[13] J.-H. Park, J.-H. Lee, Y.-H. Lee, Y.-S. Kim, J. Electron. Mater. 31 (2002) 1175–1180.
[14] M.T. Sheen, Y.H. Ho, C.L. Wang, K.C. Hsieh, W.H. Cheng, J. Electron. Mater. 34 (2005) 1318–1323.
[15] J.Y. Tsai, C.W. Chang, Y.C. Shieh, Y.C. Hu, C.R. Kao, J. Electron. Mater. 34 (2005) 182–187.
[16] Y.T. Lai, C.Y. Liu, J. Electron. Mater. 35 (2006) 28–34.
[17] J. Kloeser, E. Zakel, F. Bechtold, H. Reichl, IEEE CPMT 19A (1996) 24–33.
[18] W. Scheel: Optische Aufbau- und Verbindungstechnik in der elektronischen Baugruppenfertigung. Templin:Verlag Markus A. Detert 2002.
[19] K. Kameda, T. Azakami, M. Kameda, Nippon Kinzoku Gakkaishi 38 (1974) 434–439.
[20] J.H. Kim, S.W. Jeong, H.M. Lee, J. Electron. Mater. 31 (2002) 557–563.
[21] M. Hino, T. Azakami, M. Kameda, Nippon Kinzoku Gakkaishi 39 (1975) 1175–1181.

[22] H. Okamoto, T.B. Massalski, Bull. Alloy Phase Diagrams 5 (1984) 166–171.
[23] A. Mikula, Metall. Trans. B22 (1992) 601–611.
[24] Z. Guo, W. Yuan, M. Hindler, A. Mikula, J. Chem. Thermodyn. 48 (2012) 201–206.
[25] J.F. Elliot, J. Chipman, J. Am. Chem. Soc. 73 (1951) 2682–2693.
[26] I. Ansara, N. Dupin, in: I. Ansara, A.T. Dinsdale, M.H. Rand (Eds.), COST 507 Thermochemical Database for Light Metal Alloys, vol.2, European Comission DA XII, Luxembourg 1998.
[27] K. Kameda, S. Sakairi, Y. Yoshida, Nippon Kinzoku Gakkaishi 41 (1977) 950.
[28] R. Hultgren, P.D. Desai, D.T. Hawkins, M. Gleiser, K.K. Kelley, Selected Values of the Thermodynamic Properties of Binary Alloys (Metals Park, Ohio: ASM, 1973).
[29] E. Hayer, K.L. Komarek, J.P. Bros, M. Gaune-Escard, Z. Metallkd. 72 (1981) 109.
[30] F. Sommer, R. Lueck, N. Rupf-Bolz, B. Predel, Mater. Res. Bull. 18 (1983) 621–629.

JCT 11-275